

# Towards Accurate Time-Domain Simulation of Highly Conductive Materials

Chenghao Yuan, *Student Member, IEEE* and Zhizhang Chen, *Senior Member, IEEE*

Wireless Research Laboratory, Department of Electrical and Computer Engineering, Dalhousie University, Halifax, Nova Scotia, Canada B3J 2X4

**Abstract** — Accurate simulation of highly conductive materials such as copper at RF and microwave frequency has presented a great challenge with the conventional FDTD method. The reason is that for a FDTD recursive computation to be accurate and stable, the FDTD time step has to be very small, leading to sometimes a prohibitively large number of iterations. In this paper, the recently developed unconditionally stable ADI-FDTD method is revised and applied to solve the problem. It is shown, through the examples of computation of body of rotational (BOR) cavities with highly conductive walls, that the highly conductive materials can now be accurately simulated. In addition, a general unconditionally stable cylindrical ADI-FDTD formulation is developed to facilitate the computation of cylindrical structures with conductive loss.

## I. INTRODUCTION

The FDTD of Yee's scheme has been widely used to solve various electromagnetic problems [1]. In theory, it can be applied to compute arbitrary media including highly conductive materials. In practice, however, due to the CFL stability condition and numerical dispersion, the time step for a FDTD mesh in a highly conductive region becomes so small at RF and microwave frequencies that the number of iteration becomes prohibitively huge. As a result, approximating approaches, such as Surface Impedance Boundary Condition (SIBC) and perturbation techniques, were developed with the assumption of plane waves impinging on the conducting boundaries or unperturbed fields in the unperturbed regions [2]. These methods, though presenting good results in many cases, remain to be of approximations in nature and fail in some special cases.

The recently developed 3-D ADI-FDTD method [3][4], however, presents a potential solution for simulating highly conductive media. The reason is that the ADI-FDTD method is unconditionally stable, and allows the independent selections of time step and space step. Consequently, the ADI-FDTD becomes very suitable for solving the structures in which fine mesh is indispensable without considering the CFL condition [5]. An application of the ADI-FDTD based on this property was reported in [6] for computing shielding effectiveness of thin conductor

structures at low frequencies. Nevertheless, there has been no report on simulation of highly conductive materials at RF/Microwave frequencies. In this paper, the ADI-FDTD is extended to modeling highly conductive materials at RF and microwave frequencies. The effectiveness and efficiency of the ADI-FDTD are validated through the computations of Q-factors and resonant frequencies of body of rotational (BOR) cavities. As well, a general cylindrical ADI-FDTD formulation is developed to facilitate the computation of cylindrical structures.

This paper is organized in the following manner: Section II gives the newly developed formulation of the cylindrical ADI-FDTD for BOR structures. Section III presents the numerical results and analysis. Section IV is the summary and conclusions.

## II. NEWLY DEVELOPED FORMULATION OF CYLINDRICAL ADI-FDTD FOR THE STRUCTURES WITH CONDUCTING WALLS

Starting from Maxwell's equations, the relationship between electric field and magnetic field in the cylindrical coordinates in a lossy source free medium can be written as:

$$\epsilon \frac{\partial E_r}{\partial t} + \sigma E_r = \frac{\partial H_z}{\partial \phi} - \frac{\partial H_\phi}{\partial z} \quad (1)$$

By applying the ADI-FDTD method to the Maxwell's equations as described in [4], 12 equations can be obtained in two sub time steps respectively. For instance, equation (1) can be broken into two sub-step computation as in the following:

at the first half time step (i.e. at the  $(n+1/2)^{\text{th}}$  time step):

$$E_r^{n+1/2}(i+\frac{1}{2}, j, k) = \frac{1 - \sigma \Delta t}{4\epsilon} E_r^n(i+\frac{1}{2}, j, k) + \frac{\Delta t}{4\epsilon} \left[ \frac{H_z^{n+1/2}(i+\frac{1}{2}, j+\frac{1}{2}, k) - H_z^{n+1/2}(i+\frac{1}{2}, j-\frac{1}{2}, k)}{\Delta \phi} - \frac{H_\phi^{n+1/2}(i+\frac{1}{2}, j, k+\frac{1}{2}) - H_\phi^{n+1/2}(i+\frac{1}{2}, j, k-\frac{1}{2})}{\Delta z} \right] \quad (2a)$$

at the second half time step (i.e. at the  $(n+1)^{\text{th}}$  time step):

$$E_e^{n+1}(i+\frac{1}{2}, j, k) = \frac{1 - \frac{\sigma \cdot \Delta t}{4\epsilon}}{1 + \frac{\sigma \cdot \Delta t}{4\epsilon}} E_e^{n+1/2}(i+\frac{1}{2}, j, k) + \frac{\frac{\Delta t}{2\epsilon}}{1 + \frac{\sigma \cdot \Delta t}{4\epsilon}} \left[ \frac{H_z^{n+1/2}(i+\frac{1}{2}, j+\frac{1}{2}, k) - H_z^{n+1/2}(i+\frac{1}{2}, j-\frac{1}{2}, k)}{\Delta\phi \cdot (i+\frac{1}{2}) \cdot \Delta r} - \frac{H_y^{n+1/2}(i+\frac{1}{2}, j, k+\frac{1}{2}) - H_y^{n+1/2}(i+\frac{1}{2}, j, k-\frac{1}{2})}{\Delta z} \right] \quad (2b)$$

However, in this form, the coefficient of the field value of present time can be zero when it reaches the threshold:

$$\sigma_0 = \frac{4\epsilon}{\Delta t} \quad (3)$$

Usually this threshold conductivity value is relatively low. For example, if  $\Delta r = \Delta z = 1 \text{ cm}$ ,  $\Delta\phi = 2\pi / 20 \text{ rad}$ , taking the Courant time step limit, the threshold conductivity is  $\sigma_0 = 6.9 \text{ S/m}$ . For greater conductivity values, the coefficient will become a negative value, which makes equations (2a) (2b) unusable. To overcome this problem, Lubbers et al. [7] suggested using the most recent value of electric field in computing conduction currents. In the ADI-FDTD algorithm, it turns out to be  $\sigma E = \sigma E^{n+1/2}$  for the first half time step and  $\sigma E = \sigma E^{n+1}$  for the second half time step. As a result, the revised ADI-FDTD equations of (2a) (2b) can be derived as:

$$E_e^{n+1/2}(i+\frac{1}{2}, j, k) = \frac{1}{1 + \frac{\sigma \cdot \Delta t}{2\epsilon}} E_e^{n+1}(i+\frac{1}{2}, j, k) + \frac{\frac{\Delta t}{2\epsilon}}{1 + \frac{\sigma \cdot \Delta t}{2\epsilon}} \left[ \frac{H_z^{n+1/2}(i+\frac{1}{2}, j+\frac{1}{2}, k) - H_z^{n+1/2}(i+\frac{1}{2}, j-\frac{1}{2}, k)}{\Delta\phi \cdot (i+\frac{1}{2}) \cdot \Delta r} - \frac{H_y^{n+1/2}(i+\frac{1}{2}, j, k+\frac{1}{2}) - H_y^{n+1/2}(i+\frac{1}{2}, j, k-\frac{1}{2})}{\Delta z} \right] \quad (4a)$$

for the first half time step

$$E_e^{n+1}(i+\frac{1}{2}, j, k) = \frac{1}{1 + \frac{\sigma \cdot \Delta t}{2\epsilon}} E_e^{n+1/2}(i+\frac{1}{2}, j, k) + \frac{\frac{\Delta t}{2\epsilon}}{1 + \frac{\sigma \cdot \Delta t}{2\epsilon}} \left[ \frac{H_z^{n+1/2}(i+\frac{1}{2}, j+\frac{1}{2}, k) - H_z^{n+1/2}(i+\frac{1}{2}, j-\frac{1}{2}, k)}{\Delta\phi \cdot (i+\frac{1}{2}) \cdot \Delta r} - \frac{H_y^{n+1/2}(i+\frac{1}{2}, j, k+\frac{1}{2}) - H_y^{n+1/2}(i+\frac{1}{2}, j, k-\frac{1}{2})}{\Delta z} \right] \quad (4b)$$

for the second half time step

Note the threshold conductivity disappears in the revised equations. In this way, the revised ADI-FDTD method can be applied to the materials with high conductivities. In fact the revised ADI-FDTD is also feasible for the materials with low conductivities, as will be shown later. In the following section, numerical verification is presented to prove the validity of the revised

ADI-FDTD algorithm for the materials with both high conductivity and low conductivity.

### III. NUMERICAL VERIFICATIONS

In this section, two sample structures are computed with the revised ADI-FDTD algorithm: one is a cylindrical cavity with copper enclosure and the other is a cylindrical cavity with lossless walls filled with a slightly lossy medium. Detailed comparisons of resonant frequencies and Q-factors with the theoretical results are also presented.

#### A. Cylindrical Cavity with High Conductivity Walls

Fig. 1 shows the hollow cylindrical cavity under study. Since Q-factor is a parameter that measures the losses in a certain structure, it is used as the quality to be computed with the ADI-FDTD. For the hollow cavities, there only exists conducting loss that needs to be taken into account for the computation of the Q-factors.

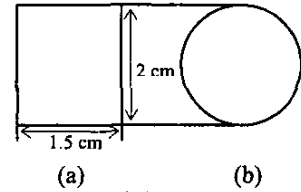


Fig. 1. The geometry of the selected cylindrical cavity: (a) Side view (b) Bottom view

To effect the realistic computation without losing modeling accuracy, the thickness of the conducting wall should be finite. In our case, a conducting layer beneath the air-conductor interface with a thickness of several times of the skin depth is taken to represent the whole conducting wall in computations of conducting loss. The justification is that the fields further down after the layer in the conductor are supposedly to be negligible small due to the strong skin depth effect at RF and microwave frequencies. In our case, we took a layer of three times of the skin depth obtained with the lowest frequency under interest as the thickness of the conductor. For the sample structure, the lowest frequency is about 11 GHz and thus the skin depth is about 0.63 μm. The thickness of the conductor was then taken to be 2.0 μm (see Fig. 2).

To reduce local numerical errors, a gradually decreased cell size is applied to the air-filled area and a uniform fine grid to the metal area in the radial direction and the z-direction, respectively (see Fig.2). The minimum cell size in the air filled area is equal to the cell size in the conducting region. The adjacent cell sizes in the air-filled area have the following relationship [1]:

$$\begin{aligned} 0.5\Delta r_{i-1} &= \Delta r_i = 2\Delta r_{i+1} \\ 0.5\Delta z_{k-1} &= \Delta z_k = 2\Delta z_{k+1} \end{aligned} \quad (5)$$

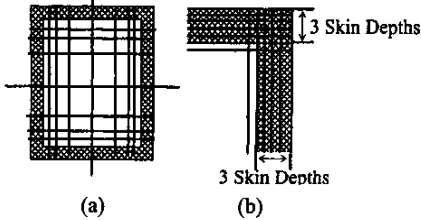


Fig. 2. (a) Non-uniform mesh in the air-filled area (b) Uniform fine mesh inside the conducting walls

Note that the first cell starts at the center of the cavity in the  $z$ -direction, and the relationship in (5) applies in both radial and  $z$ -direction. In the angular direction, a uniform mesh is used due to its homogeneousness in the direction.

With the meshing method described above, a  $50 \times 8 \times 100$  grid was generated. By recording the time domain signature at a certain grid point in the structure and then using FFT, the mode frequencies can be obtained. The unloaded Q-factor of each mode can then be calculated with:

$$Q_0 = \frac{f_o}{\Delta f} \quad (6)$$

where  $f_o$  is a certain resonant frequency and  $\Delta f$  is the corresponding 3-dB bandwidth.

In order to get correct  $\Delta f$  in (6), an appropriate frequency resolution is required. In other words, sufficient simulation duration in time is necessary with the FFT method. For a high Q structure, the 3-dB bandwidth is usually very small compared to the center frequency. This means that a high number of iteration is required. For example, if we use conventional FDTD and applying the fine mesh described above, the time step is  $7.68 \times 10^{-5}$  picoseconds at most (due to the CFL limit). To get a 1 MHz frequency resolution, 1.3 billion iterations are required, which makes the conventional FDTD impractical for calculating the Q-factor. In addition, since too many iteration steps are needed to collect enough time domain information, the calculated Q-factor is unrealistically high due to the computer-generated errors with conventional FDTD method [8].

With the unconditionally stable ADI-FDTD method the time step is only restricted by numerical accuracy. In our case the time step is taken to be 1.26 picoseconds, about 16380 times of that with the conventional FDTD.

However, even with this large time step, it still needs 800,000 iterations to get 1MHz frequency resolution. Therefore it is desired to find other techniques that can further enhance the frequency resolution with less time domain data.

There are several methods that can provide good frequency resolution with less time domain data, such as Prony's method, the generalized pencil-of-function method and FFT/Padé method. Since the first two methods are sensitive to the sampling condition [9], the FFT/Padé approximation is applied to process the FFT outputs. The detailed description of FFT/Padé method can be found in [9].

Fig. 3 illustrates the improvement of FFT/Padé method compared to FFT method with only 4,096 time domain samples with the ADI-FDTD method. The original frequency resolution is 194 MHz. The greatly refined frequency resolution is 0.13 MHz. As a result, the Q-factors are obtainable with much fewer iterations. It should be noted that even if with the FFT/Padé method, the conventional FDTD is difficult to implement since it still needs at least 1.2 million iterations.

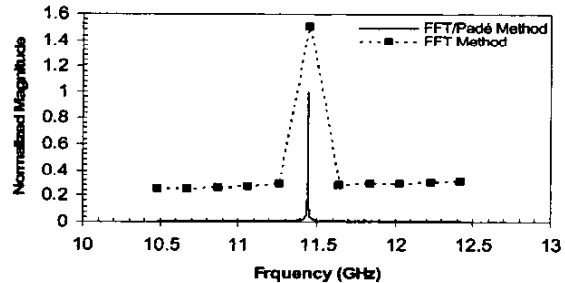


Fig. 3. The comparison between FFT and FFT/Padé method for a certain mode with the cylindrical ADI-FDTD method

Table I shows the computed resonant frequencies of a few modes and their comparisons with the theoretical values [10].

TABLE I  
RESONANT FREQUENCIES WITH PRESENTED  
METHODS

Modes	In theory (GHz) [10]	This work (GHz)	Relative Difference (%)
TM <sub>010</sub>	11.483	11.442	+0.35
TE <sub>111</sub>	13.314	13.114	+1.50
TM <sub>011</sub>	15.227	15.185	+0.28
TM <sub>110</sub>	18.300	17.781	+2.84

Table II shows the Q-factor of each mode and the comparisons with the theoretical values. As can be seen, the computed results well agree with the theoretical ones.

TABLE II  
Q-FACTOR OF EACH MODE WITH PRESENTED  
METHODS

Modes	In theory [10]	This work	Relative Difference (%)
TM <sub>010</sub>	9729	9829	-1.03
TE <sub>111</sub>	10868	11152	-2.61
TM <sub>011</sub>	8002	8100	-1.22
TM <sub>110</sub>	12281	12571	-2.36

*B Cylindrical Cavity Filled with Lossy Medium*

Dielectric loss is another kind of loss in a certain microwave structure where lossy dielectric materials exist in the structure. This kind of loss is caused by the effective conductivity of the dielectric material, which is related to the loss tangent through:

$$\sigma_{\text{eff}} = \omega \epsilon \tan \delta \quad (7)$$

Usually the effective conductivity of a lossy dielectric is of small value. For instance, the loss tangent of silicon at 10 GHz is 0.004. The effective conductivity is thus 0.0264 S/m obtained with (7).

To test the suitability of the proposed ADI-FDTD method for computing dielectric loss, an experiment is conducted for a cylindrical cavity of 210mm in diameter and 25.4mm in height with lossless walls, filled with a slightly lossy medium. The conductivity is  $\sigma = 0.001 \text{ S/m}$  at the resonant frequency.

Because the fine mesh is no longer necessary for computing this structure, a uniform  $16 \times 16 \times 15$  mesh is applied to the whole computation area. The time step is four times of the CFL limit, which is 13.0 picoseconds. Again FFT/Padé method is used to obtain frequency response as well as Q-factor. Table III shows the simulation results of TM<sub>010</sub> mode. As can be seen, the revised ADI-FDTD method is also effective for computing the low conductivity materials.

TABLE III Q-FACTOR OF TM<sub>010</sub> MODE WITH  
PRESENTED METHOD

	In theory [11]	This work	Relative Error
Q-factor	60.81	60.52	+0.47%
$f_o$ (MHz)	1093.6	1092.6	+0.09%

III. CONCLUSIONS

A revised cylindrical ADI-FDTD algorithm combined with FFT/Padé method is presented for accurately

computing the BOR structures with highly conductive walls. The proposed unconditional stable method is found to be efficient and effective in computing the loss for both high conductivity materials and low conductivity materials.

The unconditional stable ADI-FDTD method in this paper can be further extended to predict the loss of more complex structures, such as highly conductive thin film structures and attenuation loss of transmission lines.

ACKNOWLEDGEMENT

The authors acknowledge the financial support for this work from the National Science Research Council of Canada.

REFERENCES

- [1] A. Taflove, *Computational Electrodynamics: The Finite-Difference Time-Domain Method*, Boston: Artech House, 1995.
- [2] C. Wang, B. Q. Gao, and C. P. Deng, "Accurate Study of Q-Factor of Resonator by a Finite-Difference Time-Domain Method," *IEEE Trans. MTT*, vol. 43, no. 7, pp. 1524-1528, July 1995.
- [3] F. Zhen, Z. Chen, and J. Zhang, "Toward the Development of a Three-dimensional Unconditionally Stable Finite-difference Time-domain Method," *IEEE Trans. MTT*, vol. 48, no. 9, pp. 1550-1558, September 2000.
- [4] T. Namiki, "3-D ADI-FDTD Method-Unconditionally Stable Time-Domain Algorithm for Solving Full Vector Maxwell's Equations," *IEEE Trans. MTT*, vol. 48, no. 10, pp. 1743-1748, October 2000.
- [5] F. H. Zheng and Z. Z. Chen, "Numerical dispersion analysis of the unconditionally stable 3-D ADI-FDTD method," *IEEE Trans. Microwave Theory Tech.*, vol. 49, no. 5, pp. 1006-1009, May 2001.
- [6] T. Namiki, K. Ito, "Numerical Simulation Using ADI-FDTD Method to Estimate Shielding Effectiveness of Thin Conductive Enclosures," *IEEE Trans. MTT*, vol. 49, no. 6, pp. 1060-1066, June 2001.
- [7] R. J. Lubbers, and F. Hunsberger, and K. S. Kunz, "Application of a New FDTD Formulation to Highly Conductive Materials," *Proc. URSI Nat. Radio Sci. Meet.*, San Jose, CA, June 1995.
- [8] K. Chamberlin, and L. Gordon, "Modeling Good Conductors Using the Finite-Difference Time-Domain Technique" *IEEE Trans. Electromagnetic Compatibility*, vol. 37, pp. 210-216, May 1995.
- [9] Z. Ma, Y. Kobayashi, "Analysis of Dielectric Resonators Using the FDTD Method Combined with the Padé Interpolation Technique," *1999 Microwave Conference Asia Pacific*, vol. 2, pp. 401-404, September 1999.
- [10] Y. Gao, and C. J. Railton, "Efficient Determination of Q Factor by Structured Nonorthogonal FDTD Method," *Electronics Lett.*, vol. 34, no. 19, pp. 1834-1836, September 1998.
- [11] R. E. Collin, *Field Theory of Guided Waves*, New York: McGraw-Hill, 1960.